Available online at www.sciencedirect.com
SCIENCE DIRECT
Polymer 46 (2005) 3006–3013
polymer
www.elsevier.com/locate/polymer

Synthesis and rheological properties of polystyrene/layered silicate nanocomposite

Yu Zhong, Zhiyong Zhu, Shi-Qing Wang*

Maurice Morton Institute of Polymer Science and Department of Polymer Science, University of Akron, Akron, OH 44325-3909, USA

Received 1 November 2004; received in revised form 4 February 2005; accepted 9 February 2005
Available online 3 March 2005

Abstract

Exfoliated polystyrene (PS)/organo-modified montmorillonite (MMT) nanocomposites were synthesized through in situ free radical bulk polymerization by dispersing a modified reactive organophilic MMT layered silicate in styrene monomer. The original MMT was modified by a mixture of two commercial cationic surfactants, [2-(acryloyloxy)ethyl](4-benzoylbenzyl)dimethylammonium bromide (ADAB) and cetyltrimethylammonium bromide (CTAB), with the former containing a polymerizable vinyl group. The exfoliating and intercalating structures were probed by X-ray diffraction (XRD) and transmission electron microscopy (TEM). Comparing with pure PS, the nanocomposites show much higher decomposition temperature, higher dynamic modulus, stronger shear thinning behavior and a smaller die swell ratio. The leveling-off of the storage modulus at low frequencies in the oscillatory shear measurements, as well as the observed yield like behavior, implies that the formation of a percolating nanoclay network is the origin of the enhanced viscoelasticity in these composites.

Keywords: Synthesis; Rheology; Nanocomposites

1. Introduction

For a decade since the pioneering work on nylon [1,2], considerable research has been carried out to prepare polymer/clay nanocomposites (PCNs) that exhibit significantly improved thermo-mechanical properties, enhanced barrier properties and reduced flammability at rather low clay loadings [3–5]. Among many types of nanoclay used to prepare PCNs, montmorillonite (MMT) attracts most attention mainly due to their natural availability. MMT is a 2:1 mica type layered silicate, which consists of two-dimensional layers with layer thickness of around 1 nm and lateral dimension ranging from 300 Å to several microns [5]. In order to incorporate the silicate into a polymer matrix, the hydrophilic silicate is usually modified with organic quaternary ammonium salt (surfactant) through ion exchange reaction between the interlayer inorganic cations (Na^+, Ca^{2+}) and the organic cations. After the modification, the surface of silicate becomes hydrophobic, and the interlayer distance (gallery) is expanded so that polymer chains can be inserted.

Different strategies have been used to prepare PCNs. Solution blending and melt intercalation usually result in intercalated nanocomposites, where the polymer chains are inserted between silicate layers but the well ordered multilayer morphology of the clay is still present [6–12]. The exfoliated clay structure, where the silicate layers are completely delaminated into single sheets and randomly orientated in polymer matrix, could be possibly achieved through in situ polymerization [13,14]. Weimer et al. first reported a successful strategy to achieve exfoliated polystyrene/layered silicate nanocomposites by in situ controlled free radical polymerization [15]. They modified MMT by making and anchoring the nitroxyl-based organic cation, which is known for the ability to mediate the controlled 'living' free radical polymerization, on the silicate surface. Huang and Brittain synthesized exfoliated poly(methyl methacrylate) (PMMA)/clay nanocomposites through in situ suspension and emulsion polymerization [16]. For their suspension polymerization, several kinds of

* Corresponding author. Tel.: +1 330 972 7108.
E-mail address: swang@uakron.edu (S.-Q. Wang).

0032-3861/$ - see front matter © 2005 Elsevier Ltd. All rights reserved.
doi:10.1016/j.polymer.2005.02.014

modifiers were used to change the surface of layered silicate, and the organically modified silicates were used as suspension stabilizers. For the emulsion polymerization strategy, the advantage is that the original silicate does not require modification. Surfactants with a functional group, such as a vinyl group or acrylic group, can be employed to modify the clay, and they participate in the polymerization reaction, which substantially increases the compatibility between the clay and the polymer matrix and usually leads to well exfoliated nanocomposites. Fu and Qutubuddin synthesized a functional cationic surfactant vinylbenzyldimethyldodecylammonium chloride (VDAC) to modify the clay surface and achieved exfoliated PS/clay nanocomposites through in situ free radical bulk polymerization [17,18]. Zeng and Lee also obtained exfoliated PMMA or PS/layered silicate nanocomposites through in situ free radical bulk polymerization [19]. They also had to synthesize a cationic surfactant, 2-methacryloyloxyethyl-hexadecyldimethylammonium bromide (MHAB), which contains an acrylic group at one end of the chain branches, to modify the clay surface.

In this study, we employ a mixture of two surfactants, both commercially available with one containing a functional group, to modify the montmorillonite clay and to achieve exfoliated PS/clay nanocomposites through in situ free radical bulk polymerization. The structure of the two surfactants, CTAB and ADAB, are shown in Scheme 1. The utility of the long alkyl chain CTAB is to expand the gallery of MMT clay and increase the compatibility with PS. Exfoliated PS/clay nanocomposites have been made at different loadings, where the exfoliated structure was verified by the X-ray diffraction (XRD) and transmission electron microscopy (TEM) as described below.

One of the most convenient methods to elucidate the state of dispersion of PCNs is linear viscoelastic characterization. There are only a handful of studies correlating the dynamic and structural properties in intercalated nanocomposites [5,20–29]. The influence of fillers on the linear viscoelasticity of PCNs is two fold: (1) potentially modifying the polymer dynamics near the filler surfaces, and (2) forming network among the sheet-like MMT through intercalation and/or exfoliation. The purpose of the present work is to report in situ free radical bulk polymerization of exfoliated PS/clay nanocomposites and their rheological characteristics including oscillatory shear, stress relaxation and capillary flow behavior.

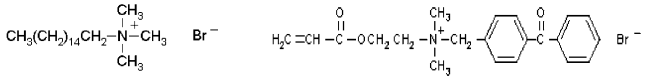

Cetyltrimethylammonium bromide (CTAB)

[2-(Acryloyloxy)ethyl](4-benzoylbenzyl) dimethylammonium bromide (ADAB)

Scheme 1. Surfactants used to modify the MMT clay.

2. Experimental

2.1. Materials

The natural montmorillonite clay used in this study, Cloisite Na^+, was provided by Southern Clay Products, with the cation exchange capacity (CEC) of 90 meq/100 g. Styrene, 2,2-azobis(isobutyronitrile) (AIBN), cetyltrimethylammonium bromide (CTAB), [2-(acryloyloxy) ethyl](4-benzoylbenzyl) dimethylammonium bromide (ADAB), and other organic chemicals and solvents were purchased from Sigma-Aldrich Chemical Co. For comparison, a commercial polystyrene from Dow Chemicals (STYRON® 678C-W) was also employed to solution-mix with commercial clays.

2.2. Modification of Cloisite Na^+

Organophilic clay was obtained after the Cloisite Na^+ was treated with CTAB and ADAB (1:1, mol/mol) through ion-exchange process. Cloisite Na^+ was first dispersed in deionized water under ultrasound for 24 h. The 1:1 (mol/mol) mixture of CTAB and ADAB was prepared in deionized water separately, and was added to the clay dispersion at an amount a little higher than the CEC of Cloisite Na^+. The resulted suspension was intensively stirred for 2 h, and was then filtered by Busch filters and washed with deionized water three times. The final product was dried in vacuum oven at room temperature for 48 h and grounded into powder.

2.3. Preparation of PS/Clay nanocomposites

Certain amount of the modified Cloisite Na^+ mentioned above and initiator AIBN were added into the styrene monomer. After exposure under ultrasound for ca. 30 min, the mixture becomes a transparent gel, which was then heated to 80 °C in an oil bath for 12 h to complete the polymerization.

For comparison, PS/clay nanocomposites were also prepared with commercial PS matrix (STYRON® 678C-W) by a solution blending method. Certain amount of the modified Cloisite Na^+ described above and STYRON® 678C-W were dissolved in toluene with ultrasound assisting for 48 h. The toluene was then evaporated. After drying in vacuum oven for another 48 h, a PS/clay nanocomposite was obtained.

2.4. Methods for characterization

Wide-angle X-ray diffraction (WAXD) analysis was performed in Professor S. Z. D. Cheng's lab on a Rigaku diffractometer equipped with a rotating-anode generator system based on the Cu Kα radiation at $\lambda = 1.5418$ Å. The slit width was 0.15 mm. The operating current was 150 mA, and the voltage was 50 kV. The scanning rate was 1°/min.

Bright-field TEM images were obtained with an FEI TECNAI-12 electron microscope operated at 120 KV. The samples were cut to 60 nm thick with a diamond knife. The thermogravimetric analysis (TGA) was performed on a Hi-Res TGA 2950 thermogravimetric analyzer (TA Instruments) in a temperature range of 30–800 °C at a heating rate of 20 °C/min in air. Molecular weight analysis was carried out by gel permeation chromatography (GPC) calibrated with standard PS samples. Before the GPC analysis, PS/clay nanocomposites were dissolved in THF and were filtered through a 0.2 μm filter in order to remove the clay structure and the clay-bounded PS.

A strain-controlled dynamic mechanical spectrometer (ARES) was used to measure the linear and nonlinear viscoelastic response of the PS/clay nanocomposites. The ARES was equipped with a 200–2000 g cm dual range force rebalance transducer, and oscillatory shear measurements were carried out at frequencies from 0.1 to 100 rad/s and temperatures from 150 to 300 °C, with a parallel plate flow cell of 8 mm in diameter. To study the yield behavior of the nanocomposites, a controlled-stress rheometer was employed. For the present work, the creep measurements were performed using a Bohlin-CVOR rheometer operated in the creep and recovery mode (equipped with 15 mm parallel plates). The testing temperature was 180 °C. A pressure controlled Monsanto Automatic Capillary Rheometer (MACR) was employed to characterize the capillary flow and die swell behavior with an aluminum die of $D=3$ mm and aspect ratio $L/D=15$. The apparent shear stress on the die wall is computed according to $\sigma=(D/4L)P$, where P is the piston pressure. The apparent shear rate on the die wall is calculated according to $\dot{\gamma}=32Q/\pi D^3$ without the Rabinowitsch correction, in which the flow rate Q is obtained by collecting and weighing the extrudate during a specific time slot. An NEC color CCD camera (NC-15D) fitted with GO Edmund Industrial Optics #53-301 close-up zoom lens was used to measure the diameter of the extrudate D' at 10 mm away from the die exit. The extrudate swell ratio (ESR) is calculated as $\mathrm{ESR}=D'/D$.

3. Results and discussions

3.1. Synthesis of PS/clay nanocomposites via in situ polymerization

Cationic surfactants, usually bulky alkylammoniums salt or alkylphosphoniums, are often used to intercalate layered silicates as well as render the virgin hydrophilic clay sufficiently compatible with organic matrices [5,30]. In order to prepare PS/clay nanocomposites, we first modified the original MMT clay, Cloisite Na^+, with a mixture of two surfactants, ADAB and CTAB, in water medium. CTAB surfactants were used to open up the gallery between clay layers because of their long hydrophobic alkyl chain tails. ADAB contains an acrylic group. It can be copolymerized with styrene monomer through AIBN initiation so that there are chemical bonds formed between the dangling reactive surfactants on the clay surface and the polymer matrix. This copolymerization of ADAB with styrene has been directly verified by solution polymerization of styrene with ADAB at a weight ratio of 1:1 in chloroform, which produced an ionomer that shows gel-like behavior with storage and loss moduli G' and G'' being parallel to each other, as shown in Fig. 1.

Fig. 2 shows the average interlayer spacing d_{001} of the clay before and after treatment with ADAB and CTAB at 1:1 molar ratio. d_{001} is seen to increase from 1.13 to 1.64 nm after the grafting of the mixed surfactants. TGA test on the modified clay also shows the amount of the surfactant in the clay gallery is close to the value calculated according to the CEC of the clay, implying that most Na^+ ions located between the galleries of clay layers have been exchanged by the surfactants.

In situ free radical bulk polymerization was carried out by dispersing 4, 6 and 9 wt% modified clay and 0.3 wt% AIBN initiator into styrene monomer and reacting at 80 °C for 12 h. The same reaction was also carried out in absence of any clay. The resulting nanocomposite is a transparent solid at clay loadings of 4 and 6%, and is translucent at a clay loading of 9%. As shown in Fig. 2, there is no diffraction peak in the XRD pattern of 4% clay loading sample when 2θ is larger than 2°, suggesting exfoliated clay dispersion in the PS matrix, or the clay layers has been pushed apart to be larger than 4.52 nm. There are hardly any visible peaks for the 6 and 9% loadings, which indicated that there is a good level of exfoliation. The exfoliated clay structure in 4% PS/clay nanocomposite is also verified with transmission electron microscopy (TEM) as shown in Fig. 3.

The molecular weight (MW) and molecular weight distribution (MWD) of the unbounded PS chains in the PS/clay nanocomposites were examined and shown in Fig. 4. To obtain the free PS for the GPC measurement, the nanocomposite sample was dissolved in THF in dilution. The solution passed through a 0.2 μm filter, which should

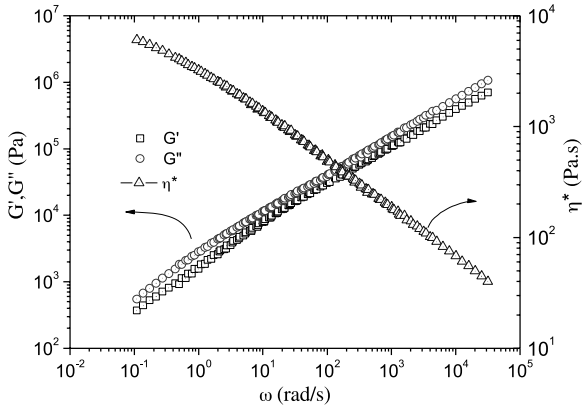

Fig. 1. Master curves for storage and loss moduli G' and G'' of the copolymer of ADAB and styrene by solution polymerization. The reference temperature is 150 °C, the temperature range is from 100 to 170 °C.

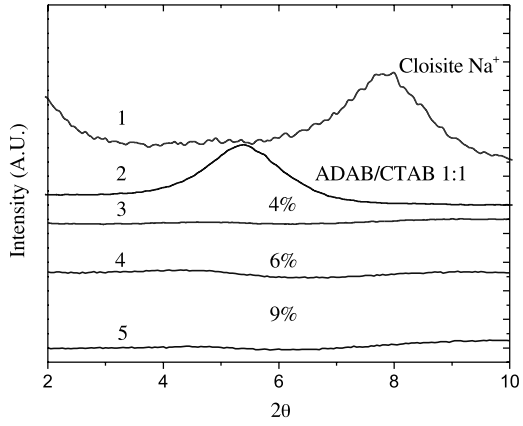

Fig. 2. X-ray diffraction spectra for (1) Cloisite Na^+, $d_{001}=1.13$ nm; (2) Cloisite Na^+ modified by ADAB/CTAB at 1:1, $d_{001}=1.64$ nm; In situ polymerized PS/clay nanocomposites at weight fractions of 4% (3), 6% (4) and 9% (5).

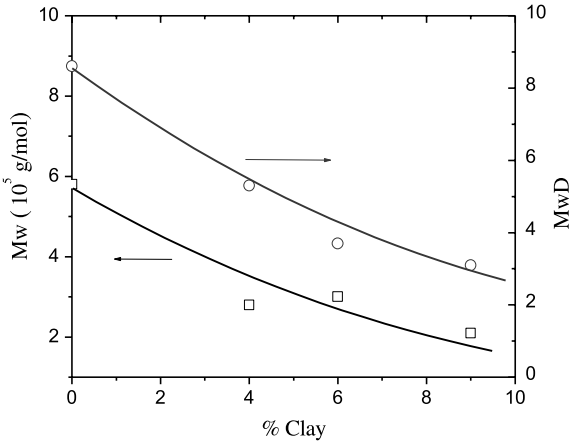

Fig. 4. Molecular weight and molecular weight distribution of PS/clay nanocomposites as well as the pure PS by in situ free radical bulk polymerization.

filter out any clay particles in the solution. Fig. 4 suggests that the presence of exfoliated clay particles has a significant effect on the polymerization characteristics. With increasing clay loading, the MW decreases and the MWD narrows, consistent with earlier results reported in literature [1,17]. Since layered silicates have already been well dispersed in the monomer matrix to form transparent gel, which is a high viscosity environment, the movement and diffusivity of the monomers, initiators and free radicals may be all retarded, and the probability of chain propagation, chain transfer and termination decreases with the clay loading.

3.2. Thermal stability

The thermal stability of the 4, 6 and 9% PS/clay nanocomposites has been characterized through TGA in air from 30 to 800 °C and compared with the pure PS in Fig. 5. As shown in Fig. 5, all the PS/clay nanocomposites exhibit much higher decomposition temperature than the pure PS. At 50% weight loss, the TGA traces of all nanocomposites show more than 50 °C shift towards higher temperature comparing with the pure PS. However, there is no significant difference from clay loading of 4–9%, suggesting there is a threshold clay loading, above which the enhancement of thermal stability saturates. Similar enhancement in thermal stability of intercalated and exfoliated PS/clay nanocomposites have been reported earlier [16,17,31,32]. Many factors could contribute to the enhancement of thermal stability in nanocomposites as indicated previously [3]. We also noticed that there was slight second-stage decomposition for the nanocomposites at ca. 430 °C, which is likely due to the loss of the surfactants ADAB and CTAB anchored on the clay layers.

3.3. Linear viscoelasticity

Fig. 6(a) presents the master curves of storage modulus G' and loss modulus G'' at a reference temperature of 150 °C for the in situ polymerized PS/clay 4% nanocomposite and for the pure PS. The master curves were obtained using time-temperature superposition (tTs) of oscillatory shear measurements between 150 and 300 °C. All the measurements were conducted with the shear amplitude of 0.5%,

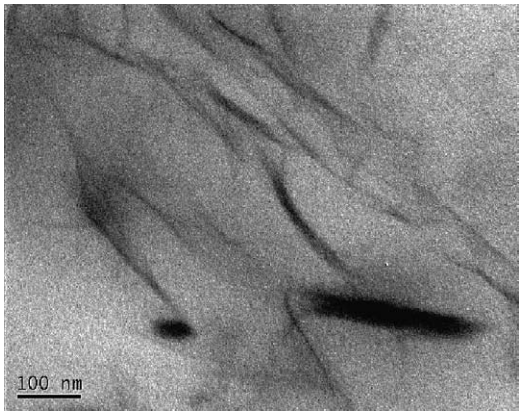

Fig. 3. TEM of in situ polymerized PS nanocomposite with Cloisite Na^+ modified by ADAB/CTAB at 1:1.

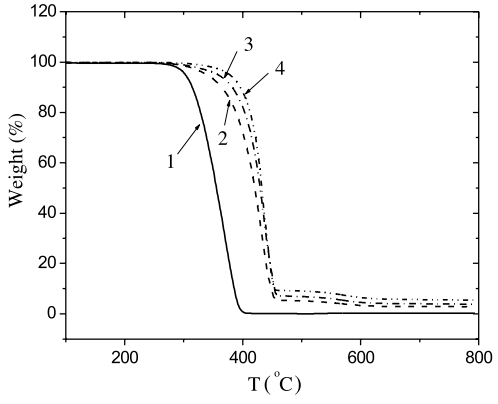

Fig. 5. Percentage weight loss in TGA measurements of (1) Pure PS; PS/clay nanocomposite with 4% (2), 6% (3) and 9% (4) clay loading.

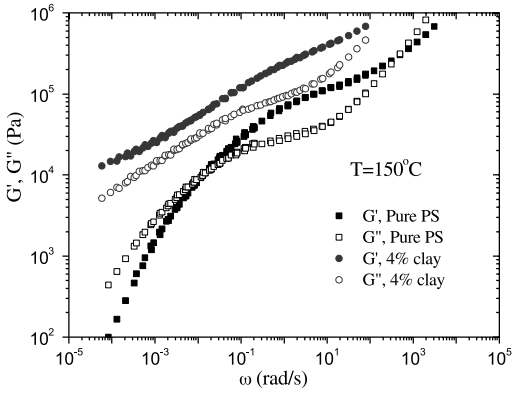

(a)

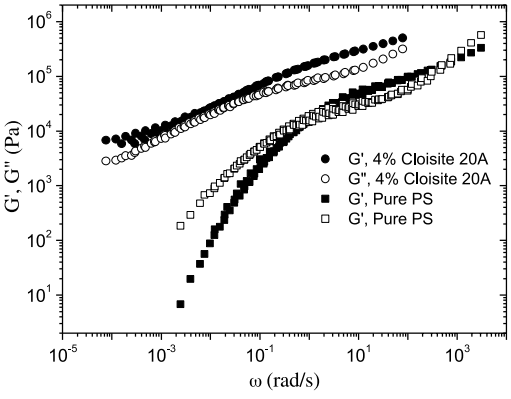

(b)

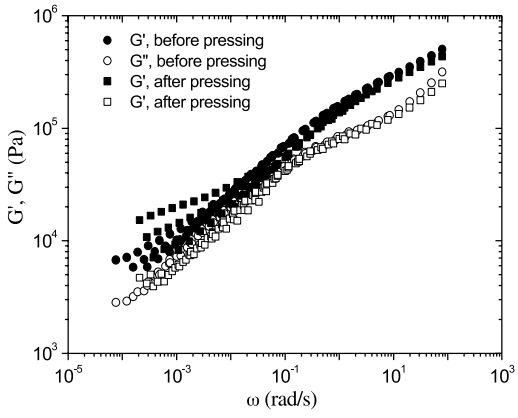

(c)

Fig. 6. (a) Master curves for storage and loss moduli G' and G'' of pure PS and PS/clay 4% nanocomposite (in situ polymerization) at 150 °C. (b) Master curves of PS/clay 4% nanocomposite (solution-blending based on a commercial PS) at 150 °C. (c) G'' and G'' of the solution-blended sample of (b) before and after melt pressing at 300 °C.

which is in the linear viscoelastic region of the nanocomposite, to avoid the shear induced alignment of silicate layers. As a comparison, similar master curves of G' and G'' for an intercalated PS/clay 4% nanocomposite made from solution blending is shown in Fig. 6(b).

Several comments on Fig. 6(a) and (b) are in order. Both Fig. 6(a) and (b) show that G' and G'' are parallel to each other, with $G' > G''$ throughout the explored frequency range. The *t*Ts principle has been applied before for nanocomposites [22–24,33], and was found to be applicable for the current in situ polymerized 4% PS/clay nanocomposite. In contrast, the PS/clay 4% nanocomposite made from solution blending reveals a failure of *t*Ts, indicating some possible structure changes above 250 °C, e.g. the desorption of polymer chain from the surface of silicate layers and the re-orientation of silicate layers. This fact confirms the advantage of using a mixture of reactive and long alkyl chain surfactants, which significantly increase both interaction and compatibility between the silicate layers and polystyrene matrix so that the nanocomposite by in situ polymerization is more thermally stable than that by solution blending.

Secondly, as shown in Fig. 6(a), the exfoliated PS/clay 4% nanocomposite tends to show leveling-off in G' and G'' and absence of crossover between G' and G'' at low frequency region, although the pure PS exhibits a clear terminal region at these low frequencies. This gel-like characteristic of the nanocomposites is due to the network structuring from the well dispersed silicate layers.

Fig. 7 shows that the complex viscosity of the 4, 6 and 9% clay loading PS nanocomposites as a function of the oscillation frequency, also based on linear oscillatory shear measurements after applying *t*Ts. The diverging complex viscosity with lowering frequency at all of the three loading is evidence that large-scale association of the sheet-like clay particles occurred even at these low volume fractions.

Stress relaxation experiments were carried out to characterize the linear rheological properties of the in situ polymerized PS/clay nanocomposites. Fig. 8(a) presents the typical stress relaxation of the pure PS at temperatures from 170 to 230 °C, and Fig. 8(b) shows the stress relaxation of the 4% PS/clay nanocomposite at temperatures from 150 to 210 °C. All the measurements employed strain amplitude of 1.0%. The comparison between Fig. 8(a) and (b) indicates that the nanocomposite has much slower relaxation times than the pure PS does, even although the latter has a higher

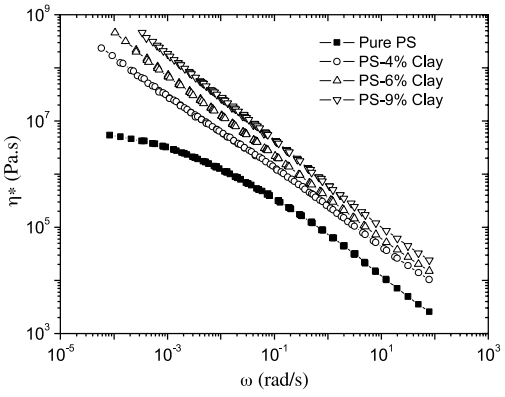

Fig. 7. Complex viscosity in a function of frequency for the pure PS and PS/clay nanocomposites at 150 °C from oscillatory shear measurements in the temperature range of 150–300 °C.

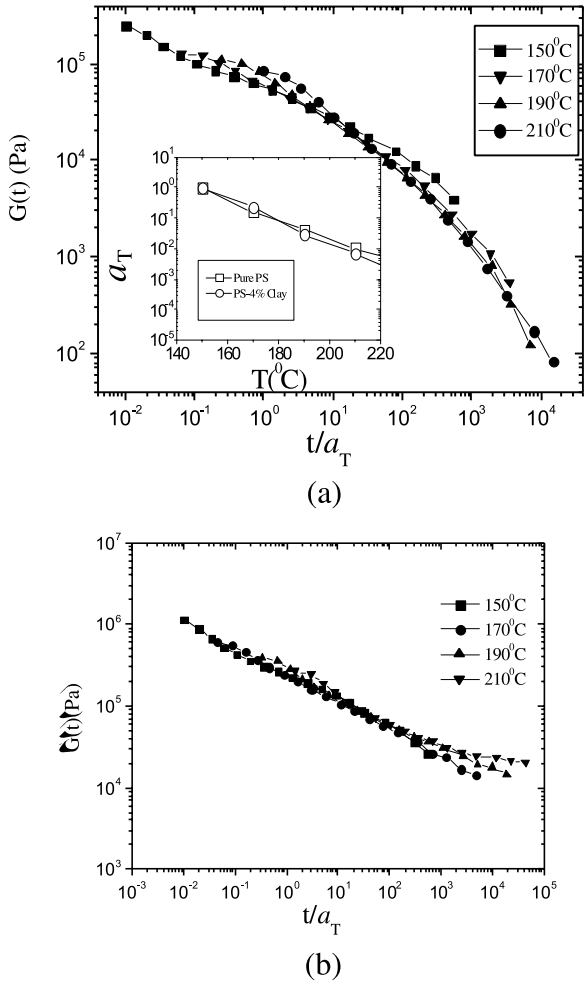

Fig. 8. (a) Stress relaxation of the pure PS at different temperatures. (b) Stress relaxation of PS/clay 4% nanocomposites at different temperatures.

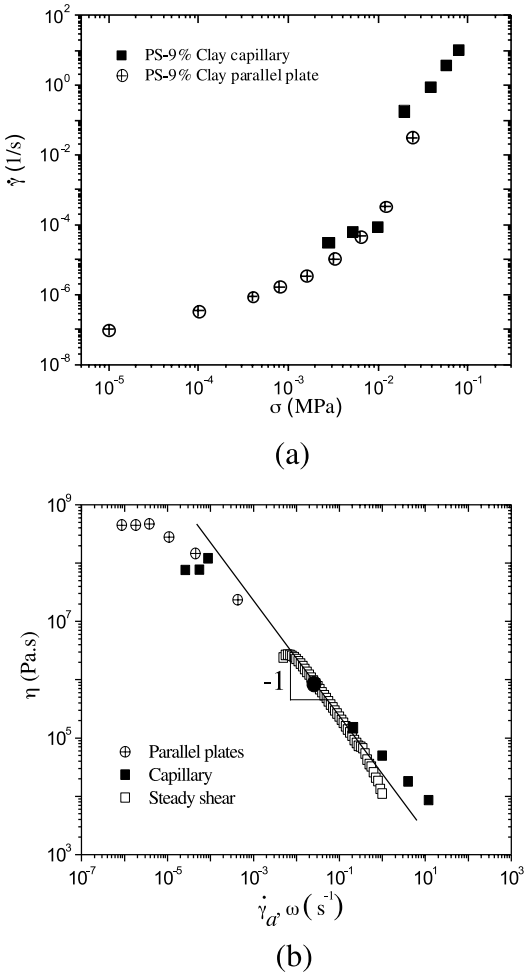

Fig. 9. (a) Yield behavior of PS/9% clay nanocomposites at 190 °C characterized in pressure-driven capillary and stress-controlled parallel-plate rheometries. (b) Steady shear viscosity as measured in both controlled stress and controlled rate modes.

MW and MWD than the matrix PS of the composite. It is more striking to see that the stress relaxation of the nanocomposite is independent of temperature in sharp contrast to the behavior of the pure PS. Clearly, the stress relaxation in the nanocomposite is not dictated by the matrix polymer relaxation, but rather depends on the relaxation of the network formed by the sheet-like clay particles, which apparently is insensitive to the temperature change.

3.4. Yield and steady shear behavior

The filler network in the well-exfoliated polymer/clay nanocomposite as indicated by the oscillatory shear behavior given in Fig. 6 would imply that they may possess yield stress [34]. Methods have been established to characterize the yield behavior of filled polymers and colloidal suspensions [35–37]. Fig. 9(a) presents the yield behavior of the 9% PS/clay nanocomposite at 190 °C using two apparatuses. The nanocomposite was extruded through a capillary die of $D=1.2$ mm and $L/D=40$ with a stress controlled rheometer, MACR. The stress was varied successively from 0.005 to 0.1 MPa. Sufficient time was used for every data point to collect the extrudate and weigh its mass to determine the flow rate Q and shear rate according to $\dot{\gamma}=32Q/\pi D^3$. The sample was also sheared in a stress controlled rheometer (Bohlin-CVOR) with 15 mm parallel-plates whose surfaces are made of sandpapers to avoid wall slip [37]. Shear stresses between 500 Pa and 50 kPa were applied. For each stress a new sample was loaded. A yield like transition was seen in both capillary and parallel plate flows. Another way of characterizing this yield behavior is to examine the sample using controlled-rate measurements and plot the steady-state shear viscosity as a function of the applied apparent shear rate. Fig. 9(b) shows such a plot along with the controlled-stress data from Fig. 9(a). The overlapping of these different sets of data confirms that the shear stress is essentially constant independent of the apparent shear rate, i.e. $\eta=\sigma/\dot{\gamma}$ scales inversely with $\dot{\gamma}$. The yield behavior in the polymer/clay nanocomposites has also been reported previously for the

intercalated system, which was attributed to the destruction of the clay percolating structure by the shearing force.

3.5. Nonlinear viscoelasticity

Polymer/clay nanocomposites exhibit nonlinear viscoelasticity at large strain amplitudes in oscillatory shear just as the conventional filled polymers do. Fig. 10 shows the storage modulus G' of pure PS and the 4, 6 and 9% clay nanocomposites at $\omega = 0.1$ rad/s and $T = 220$ °C as a function of strain amplitude γ from 0.01 to 100%. All the three nanocomposites show the well-known Payne effect [38]. The onset strain for the Payne effect is smaller for the higher clay loading, as expected.

3.6. Extrudate swell behavior

Controlling and understanding extrudate swell are crucial to processing of polymer materials including thermoplastics and rubbers. Extrudate swell behavior of polymer/clay nanocomposites has not been studied previously to our knowledge. Fig. 11 presents the extrudate swell ratio of Styron® 678C-W and the solution-blended 4, 6 and 9% PS/clay nanocomposites at 180 °C obtained from a capillary die of $D = 3.0$ mm and $L/D = 15$ at different stresses. The measurements were made at 10 mm away from the die exit with a video-camera connected to a VCR. The die swell of the nanocomposites is drastically smaller at all stresses, with the contrast particularly striking between the pure Styron® 678C-W and 9% Styron® 678C-W/clay nanocomposite. Die swell takes place because the residual stress due to the un-relaxed chain deformation causes the extrudate to rearrange its shape. It is well known that die swell grows over time and the growth rate is related to the characteristics of the relaxation dynamics [39]. Since the nanocomposites are much more viscoelastic according to Fig. 6(b), die swell take place much more slowly, relative to that of the pure PS. The extrudate cooled in time below the glass transition temperature as it moved away from the die exit, and die swell was arrested.

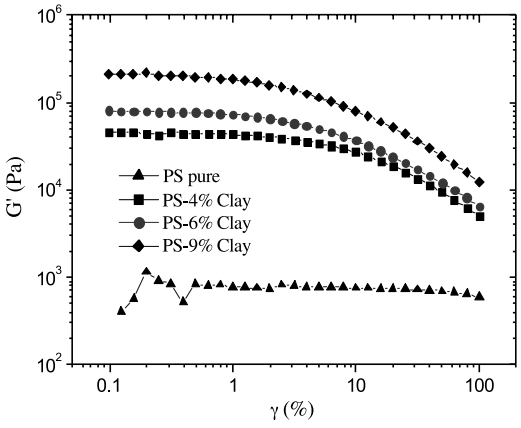

Fig. 10. Storage modulus of pure PS and PS/clay nanocomposites at 4, 6 and 9% clay loadings at 220 °C and frequency equal to 0.1 rad/s as a function of the strain amplitude.

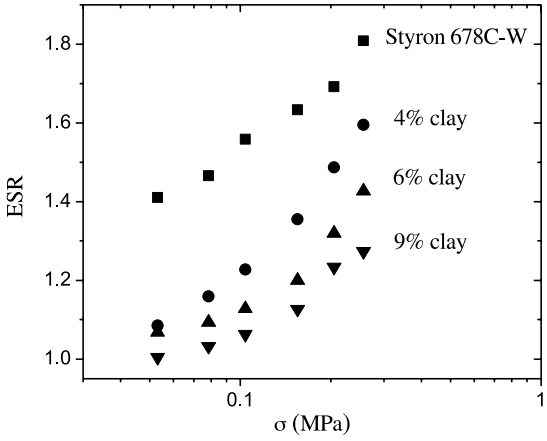

Fig. 11. Die swell of PS/clay nanocomposites measured using a Monsanto capillary rheometer at 180 °C.

4. Conclusions

In this work, we used in situ free radical bulk polymerization to prepare exfoliated montmorillonite (MMT) layered silicate based polystyrene (PS) nanocomposites. Our approach consisted of treating the MMT with a mixture of two commercial surfactants via ionic exchange. Since one surfactant possesses a polymerizable vinyl group, the in situ polymerization allowed PS to be 'grafted' onto the organo-clay sheets by co-polymerization. Such PS/clay nanocomposites can be cheaply made and are not only highly exfoliated but also stable both thermally and mechanically, in contrast to those made from solution blending of organo-clay with premade PS.

These nanocomposites were characterized with a number of experimental techniques, especially the rheological measurements including both oscillatory shear and steady-shear in both controlled stress and controlled-rate modes, in both parallel plates and capillary flow. Rheological characterization is clearly a rather convenient tool to determine not only whether a good level of exfoliation is achieved but also whether the dispersion of nanoclay is mechanically stable or not. Several interesting features of these PS/clay nanocomposites include: (a) relaxation dynamics of the materials are dominated by the clay–clay association so that the stress relaxation remains independent of temperature; (b) the nanocomposites show yield-like behavior that is normally observed only for highly filled systems; (c) the die swell of the nanocomposites is greatly reduced in comparison to that of the pure PS matrix.

Acknowledgements

This work is supported, in part, by ACS-PRF 34529-AC7 and by National Science Foundation grant (CTS 0115867). The authors also thank Professor Stephen Z.D. Cheng for generously providing X-ray diffraction facility.

References

[1] Usuki A, Kojima Y, Kawasumi M, Okada A, Fukushima Y, Kurauchi T, et al. J Mater Res 1993;8(5):1179.
[2] Kojima Y, Usuki A, Kawasumi M, Okada A, Fukushima Y, Kurauchi T, et al. J Mater Res 1993;8(5):1185.
[3] Alexandre M, Dubois P. Mater Sci Eng 2000;28(1–2):1.
[4] Vaia RA, Giannelis EP. MRS Bull 2001;5:394.
[5] Giannelis EP, Krishnamoorti R, Manias E. Adv Polym Sci 1999;138: 107.
[6] Lagaly G. Appl Clay Sci 1999;15:1.
[7] Giannelis EP. Adv Mater 1996;8(1):29.
[8] Kawasumi M, Hasegawa N, Kato M, Usuki A, Okada A. Macromolecules 1997;30(20):6333.
[9] Lan T, Pinnavaia TJ. Chem Mater 1994;6(12):2216.
[10] Vaia RA, Ishii H, Giannelis EP. Chem Mater 1993;5(12):1694.
[11] Vaia RA, Giannelis EP. Macromolecules 1997;30(25):8000.
[12] Vaia RA, Jandt KD, Kramer EJ, Giannelis EP. Macromolecules 1995; 28(24):8080.
[13] Kojima Y, Usuki A, Kawasumi M, Okada A, Kurauchi T, Kamigaito O. J Polym Sci, Part A: Polym Chem 1993;31(7):1755.
[14] Noh MW, Lee DC. Polym Bull (Berlin) 1999;42(5):619.
[15] Weimer MW, Chen H, Giannelis EP, Sogah DY. J Am Chem Soc 1999;121(7):1615.
[16] Huang X, Brittain WJ. Macromolecules 2001;34(10):3255.
[17] Fu X, Qutubuddin S. Polymer 2001;42(2):807.
[18] Qutubuddin S, Fu X, Tajuddin Y. Polym Bull (Berlin) 2002;48(2): 143.
[19] Zeng C, Lee LJ. Macromolecules 2001;34(12):4098.
[20] Krishnamoorti R, Vaia RA, Giannelis EP. Chem Mater 1996;8(8): 1728.
[21] Krishnamoorti R, Giannelis EP. Macromolecules 1997;30(14):4097.
[22] Ren J, Silva AS, Krishnamoorti R. Macromolecules 2000;33(10): 3739.
[23] Krishnamoorti R, Yurekli K. Curr Opin Colloid Interface Sci 2001; 6(5–6):464.
[24] Krishnamoorti R, Ren J, Silva AS. J Chem Phys 2001;114(11): 4968.
[25] Ren J, Krishnamoorti R. Macromolecules 2003;36(12):4443.
[26] Solomon MJ, Almusallam AS, Seefeldt KF, Somwangthanaroj A, Varadan P. Macromolecules 2001;34(6):1864.
[27] Galgali G, Ramesh C, Lele A. Macromolecules 2001;34(4):852.
[28] Mousa A, Karger-Kocsis J. Macromol Mater Eng 2001;286(4):260.
[29] Becker O, Sopade P, Bourdonnay R, Halley PJ, Simon GP. Polym Eng Sci 2003;43(10):1683.
[30] Lagaly G. Solid State Ionics 1986;22(1):43.
[31] Burnside SD, Giannelis EP. Chem Mater 1995;7(9):1597.
[32] Doh JG, Cho I. Polym Bull 1998;41(5):511.
[33] Meincke O, Hoffmann B, Dietrich C, Friedrich C. Macromol Chem Phys 2003;204(5–6):823.
[34] Malkin AY. Adv Polym Sci 1990;96:70.
[35] Barnes HA. J Non-Newtonian Fluid Mech 1999;81(1–2):133.
[36] Walls HJ, Caines SB, Sanchez AM, Khan SA. J Rheol 2003;47(4): 847.
[37] Zhong Y, Wang S-Q. J Rheol 2003;47(2):483.
[38] Payne AR. J Appl Polym Sci 1962;6:57.
[39] Zhu Z, Wang S-Q. J Rheol 2004;48(3):571.